iFuzzyTL: Interpretable Fuzzy Transfer Learning for Steady-state Visual Evoked Potentials Brain-Computer Interfaces System

Xiaowei Jiang[1†], Beining Cao[1†], Liang Ou[1], Yu-Cheng Chang[1], Thomas Do[1], Chin-Teng Lin[*1]
[1]Computational Intelligence and Brain Computer Interface Lab, School of Computer Science,
Faculty of Engineering and Information Technology, University of Technology Sydney

***Abstract*—The rapid evolution of Brain-Computer Interfaces (BCIs) has significantly influenced the domain of human-computer interaction, with Steady-State Visual Evoked Potentials (SSVEP) emerging as a notably robust paradigm. This study explores advanced classification techniques leveraging interpretable fuzzy transfer learning (iFuzzyTL) to enhance the adaptability and performance of SSVEP-based systems. Recent efforts have strengthened to reduce calibration requirements through innovative transfer learning approaches, which refine cross-subject generalizability and minimize calibration through strategic application of domain adaptation and few-shot learning strategies. Pioneering developments in deep learning also offer promising enhancements, facilitating robust domain adaptation and significantly improving system responsiveness and accuracy in SSVEP classification. However, these methods often require complex tuning and extensive data, limiting immediate applicability. iFuzzyTL introduces an adaptive framework that combines fuzzy logic principles with neural network architectures, focusing on efficient knowledge transfer and domain adaptation. iFuzzyTL refines input signal processing and classification in a human-interpretable format by integrating fuzzy inference systems and attention mechanisms. This approach bolsters the model's precision and aligns with real-world operational demands by effectively managing the inherent variability and uncertainty of EEG data. The model's efficacy is demonstrated across three datasets: 12JFPM (89.70% accuracy for 1s with an information transfer rate (ITR) of 149.58), Benchmark (85.81% accuracy for 1s with an ITR of 213.99), and eldBETA (76.50% accuracy for 1s with an ITR of 94.63), achieving state-of-the-art results and setting new benchmarks for SSVEP BCI performance.**

***Index Terms*—Brain-computer interface, SSVEP, fuzzy logic, transfer learning, attention mechanisms**

I. Introduction

BRAIN-COMPUTER interfaces (BCIs) have become increasingly popular in human-computer interaction (HCI) due to their intuitive nature[1–4]. BCIs allow for direct extraction of user intentions from the brain, bypassing the peripheral nervous system and muscle tissue[5]. Among the various non-invasive EEG-based BCI paradigms, such as steady-state visual evoked potentials (SSVEP)[6, 7], P300[8], and motor imagery (MI)[9]. SSVEP is particularly noted for its high accuracy and robustness. In SSVEP BCIs, users focus on visual stimuli flickering at different frequencies, and their intent is deciphered by identifying the frequency of the observed flicker. Remarkably, research in this field has advanced to where forty commands can be distinguished within just one second of EEG data[10].

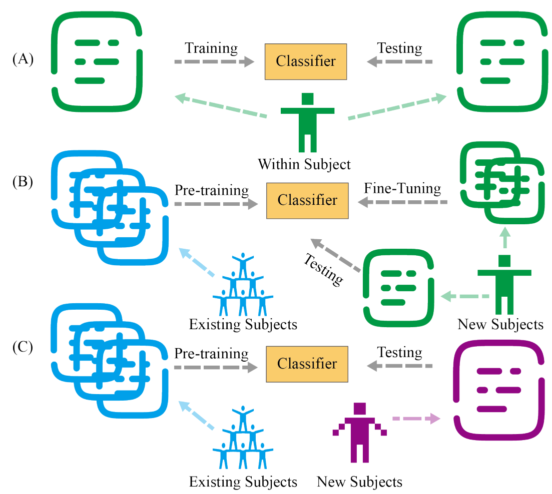

Fig. 1: The diagram of three classification scenarios. **(A)** intra-subject classification; **(B)** inter-subject few-shot classification; **(C)** inter-subject zero-shot classification.

Classification methods for SSVEP are broadly categorized into unsupervised and supervised techniques. Canonical correlation analysis (CCA)[11] and Filter-bank CCA[12] are traditional unsupervised methods that determine the target frequency by measuring the correlation between EEG signals and predefined reference signals. Although effective, their performance lags behind supervised methods, particularly with shorter EEG segments[13] in the intra-subject classification task, as shown in Fig. 1(A). Consequently, supervised methods such as extended CCA (eCCA)[14], task-related component analysis (TRCA)[15], and complex-spectrum convolutional neural networks (CCNN)[16] have been developed, significantly outperforming unsupervised approaches. However, these high-performing supervised methods require extensive data collection for model training or user-specific calibration, hindering their immediate usability[17, 18]. As a result, transfer learning has emerged as a key research area in SSVEP studies[19, 20]. This approach leverages knowledge gained from the source

[†]Xiaowei Jiang and Beining Cao contributed equally to this work.
[*]Corresponding author: Chin-Teng Lin. Email: chin-teng.lin@uts.edu.au

subjects to improve performance on new subjects [21], minimizing the need for extensive calibration typically required for personalized BCIs. Techniques such as domain adaptation are employed to modify models developed on one individual's data for use with another's, significantly enhancing cross-subject generalizability[22, 23]. In SSVEP, some transfer learning methods based on CCA using the spatial filter and templates to learn the knowledge from existing domains [13, 19] Additionally, fine-tuning deep learning models pre-trained on large datasets in a domain-specific manner can substantially reduce the discrepancy between training and implementation environments, offering a robust solution for SSVEP BCI applications[16, 24]. Hybrid strategies that combine classical signal processing with advanced machine learning techniques also play a crucial role [25–27]. These methods preprocess EEG signals to extract features more invariant across subjects before training classifiers, thereby balancing performance with computational efficiency essential for real-time applications.

Recent advances have focused on reducing the need for calibration through few-shot learning approaches, as shown in Fig. 1(B). Pioneering work by Chi Man Wong et al. introduced a subject transfer-based CCA (stCCA), which utilizes cross-subject spatial filters and SSVEP templates to enhance transferability[28]. This method achieved an impressive information transfer rate of 198.18 ± 59.12 bits/min with minimal calibration trials for a 40-target task, Benchmark[10]. Further, numerous modified CCA methods have been proposed to refine few-shot learning in SSVEP[29–32]. Alternatively, deep learning (DL) frameworks are renowned for their efficacy in utilizing previously acquired knowledge to address challenges in transfer learning and domain adaptation, effectively managing uncertainties and enhancing predictive accuracy across related domains [21, 33]. In SSVEP, DL is also being explored for their potential in few-shot SSVEP transfer learning, such as convolutional neural network (CNN)[34, 35] or Transformer-based[24], although they still necessitate some degree of calibration.

However, while few-shot learning approaches significantly reduce the reliance on extensive calibration, they do not eliminate it entirely. Consequently, the development of zero-shot learning scenarios for SSVEP is crucial, as illustrated in Fig. 1(C). Signal correlation analysis (CA) methods, such as CCA and TRCA, which leverage parameters solely from the source domain [20, 36, 37], demonstrate the capacity for zero-shot learning. While zero-shot CA methods generally underperform compared to their few-shot counterparts, DL-based transfer learning techniques, using architectures like long short-term memory (LSTM) and Transformers, have shown promising results in achieving higher accuracy[35, 38]. Despite these advancements, DL methods are often criticized for their lack of interpretability compared to the transparent calculations of CA methods[39]. Interpretability helps explain model failures and enhances system stability, therefore, developing an interpretable DL framework that elucidates the underlying mechanisms remains a critical challenge in the field.

The Fuzzy Neural Network (FNN) [40–42] stands out as a potential framework that combines the robustness of neural networks with the clarity of fuzzy logic systems. FNNs utilize fuzzy rules and membership functions to process inputs, thereby maintaining a logical structure that is both transparent and intuitive. This method contrasts sharply with more opaque models, clearly visualizing how inputs are transformed into outputs through human-understandable rules, thus helping user optimize the BCI system. Drawing on the principles of fuzzy logic [43], particularly the Takagi–Sugeno–Kang (TSK) inference systems [44], our work introduces the interpretable fuzzy transfer learning (iFuzzyTL) model—a novel Fuzzy Inference Systems (FISs) based on fuzzy set theory [44], tailored for the SSVEP task.

FISs have been further developed into a neural network architecture known as FNN, which can be trained using gradient descent optimization, providing good interpretability. A recent study, KAN [45], highlights that learning dimension-specific activation functions introduces "internal degrees of freedom," a concept naturally realized in the TSK model through centroid and width parameters, distinguishing it from linear-based models like Transformers and CNNs. One study demonstrates that introducing a Fuzzy Attention Layer significantly enhances the network's approximation capabilities by leveraging internal degrees of freedom [46]. Inspired by these findings, our model is derived from these fuzzy systems studies. It is designed to learn robust knowledge by exploiting extensive evidence and enables significant adaptation in environments characterized by limited data availability, and handle uncertainty and variability[47]. Furthermore, fuzzy rule-based transfer learning models, including ours, have demonstrated remarkable capabilities in addressing the challenges posed by small source datasets in transfer learning scenarios, ensuring reliable performance even when existing data resources are sparse [48–52], especially the application in brain signal processing [53–56], and EEG-based BCI system [57].

In addressing the challenges of domain adaptation, iFuzzyTL modifies the source domain model's input and/or output spaces through spatial transformations. This ensures that the fuzzy rules align more precisely with the target data, enhancing the model's robustness even with minimal available data. Furthermore, the capacity of fuzzy logic to cluster data and facilitate the separation of classes during the domain transfer process has been proved by unsupervised transfer learning models [49, 58, 59]. Following the idea of clustering, iFuzzyTL calculates the membership degree based on the distance between input features and the centroid of fuzzy sets. Each centroid represents a prototype characteristic of its cluster, and the distances are measured using a suitable metric, typically Euclidean[60]. The closer an input feature is to a fuzzy centroid, the higher its membership grade is to that centroid. The membership grade determines the firing strength of the fuzzy rules associated with the corresponding center, with the rule strength computed using a fuzzy operation (e.g., sum, product, min, or max) applied to the input membership grades. This approach enables the system to process inputs that exhibit varying degrees of similarity to known categories, and the nonlinearity provided by the Gaussian membership functions makes the approximation of real-world data more robust [61], thereby accommodating real-world data's inherent uncertainty and fuzziness. As a result, iFuzzyTL provides a robust, human-interpretable, and adaptable framework for applications requiring nuanced decision-making processes.

To further refine the model's capabilities, the dual-filter structure, which includes both spatial and temporal filters as applied by EEGNET [62], demonstrates significant enhancements in processing EEG data. iFuzzyTL incorporates Fuzzy Attention Layers [46] as spatial and temporal filters to capture and generalize the central fuzzy rules within the network. This architecture effectively learns the domain knowledge of both spatial and temporal dependencies in the brain signals, enabling more accurate and robust feature extraction and domain adaptation, especially in transfer learning scenarios. These filters in iFuzzyTL integrate fuzzy set theory with neural network architectures to model SSVEP signal sequences as fuzzy sets. This approach parallels the mechanism of vanilla dot-product self-attention [63–65], enhancing the robustness and flexibility of the model in neurophysiological applications. By melding fuzzy logic with advanced attention mechanisms, iFuzzyTL facilitates efficient knowledge transfer across varying domains and sets a new benchmark in the field of computational intelligence-based transfer learning, especially for tasks involving complex signal patterns like SSVEP. Our model achieves the highest ITR and accuracy in three datasets as zero-shot learning, 12JFPM(89.70% for 1s with ITR=149.58), Benchmark(85.81% for 1s with ITR=213.99), and eldBETA(76.50% for 1s with ITR=94.63), and is the State Of The Art (SOTA) model in the SSVEP transfer learning issue. We also demonstrate how the iFuzzyTL model enhances interpretability by revealing the temporal dynamics of firing strength and its harmonic relationships with target frequencies in the SSVEP task.

The contributions of this study are outlined as follows:

1) **Development of iFuzzyTL:** We introduce a novel fuzzy logic-based attention mechanism called iFuzzyTL, designed to enhance transferability in SSVEP BCI tasks. This development significantly reduces the need for user-specific calibration, facilitating a more efficient "plug-and-play" experience in BCI systems.
2) **Enhancement of Interpretability:** Our approach improves the interpretability of BCI systems by integrating fuzzy logic with neural networks. We utilize a human-understandable center for clustering and learning, which allows for clearer insights and better design of the mechanisms driving BCI technology.
3) **Advancements in Practical Usability:** The study showcases the model's enhanced capability to adapt to new subjects without the need for retraining or recalibration, markedly boosting its practical usability and reliability in various real-world settings.

II. Methods and materials

A. Explanation of SSVEP Principles and Stimulus Frequency Modulation

The principle behind SSVEP can be understood as a response of the sensory cortex to visual stimuli presented at specific frequencies, such as flicker [66] or other reversal patterns [67]. This interaction results in an oscillatory brain response at both the stimulus frequency f_s and its harmonic frequencies kf_s (where k is a positive integer) [68].

The most commonly used stimulus is flicker, whose chrominance value can be modulated sinusoidally to achieve a fixed frequency change:

$$C(t) = \begin{bmatrix}255\\255\\255\end{bmatrix} \times \left(\frac{1+\sin(2\pi f_s t+\phi)}{2}\right) \tag{1}$$

Here, $C(t)$ represents the chrominance value at time t, f_s is the frequency of the visual stimuli which can also be defined as y in the prediction task, ϕ is the phase shift, and n denotes the number of target frequencies corresponding to n stimuli. By decoding the EEG frequency response of the subject, one can infer the target f_k that the subject is focusing on, thereby revealing their intentions.

By watching the flicker and recording the EEG signal from the occipital cortex, the ideal recorded brain response $x(t)$ can be expressed as [69]:

$$x(t) = \sum_{k=1}^{n} A_k \sin(2\pi k f_s t + \theta_k) \tag{2}$$

where A_k is the amplitude of the response at each harmonic k and θ_k represents the phase associated with each harmonic frequency. This formulation highlights how the brain responds to the specific frequencies of visual stimuli, allowing for effective communication of the subject's focus.

B. Task Definition and Data Structure

We explore the domain of SSVEP tasks, incorporating data from N subjects to employ transfer learning techniques. The objective is to pretrain a model that adapts to new subjects under a zero-shot learning framework. Let $\mathcal{S} = \{\mathcal{S}_1, \mathcal{S}_2, \ldots, \mathcal{S}_N\}$ represent the source domains, with each $\mathcal{S}_n$ comprising pairs $\{(x^i_{\mathcal{S}_n}, y^i_{\mathcal{S}_n}) \mid x^i_{\mathcal{S}_n} \in X_n, y^i_{\mathcal{S}_n} \in Y\}_{i=1}^{m_n}$. The target domain $\mathcal{T}$, which consists of unlabeled samples $\{x^j_{\mathcal{T}} \in X_{\mathcal{T}}\}_{j=1}^{m_{\mathcal{T}}}$, aims to adapt using the learned knowledge from $\mathcal{S}$ to predict labels $\{y^j_{\mathcal{T}} \in Y\}_{j=1}^{m_{\mathcal{T}}}$ effectively, achieving zero-shot learning.

C. The proposed iFuzzyTL

1) Fuzzy Inference Systems and Their Attention Mechanisms: FISs play a crucial role in modeling uncertainty and imprecision in numerous fields, providing a sophisticated framework to manage complex and ambiguous data sets [70–73]. At the core of these systems lie the concepts of fuzzy sets and membership functions, where the degree of membership $\mu_A(x)$ quantifies how closely an element x conforms to a fuzzy set A. The TSK model is a prevalent form of FIS [44], characterized by its use of IF-THEN rules to articulate the relationships between inputs and outputs. Specifically, a $Zero^{\text{th}}$ order TSK system utilizes the following rule structure:

$$\text{If } x_1 \text{ is } A_{1,r} \text{ and } \ldots \text{ and } x_D \text{ is } A_{D,r}, \tag{3}$$

$$\text{then } y = u_r, \quad r = 1, \ldots, R, \tag{4}$$

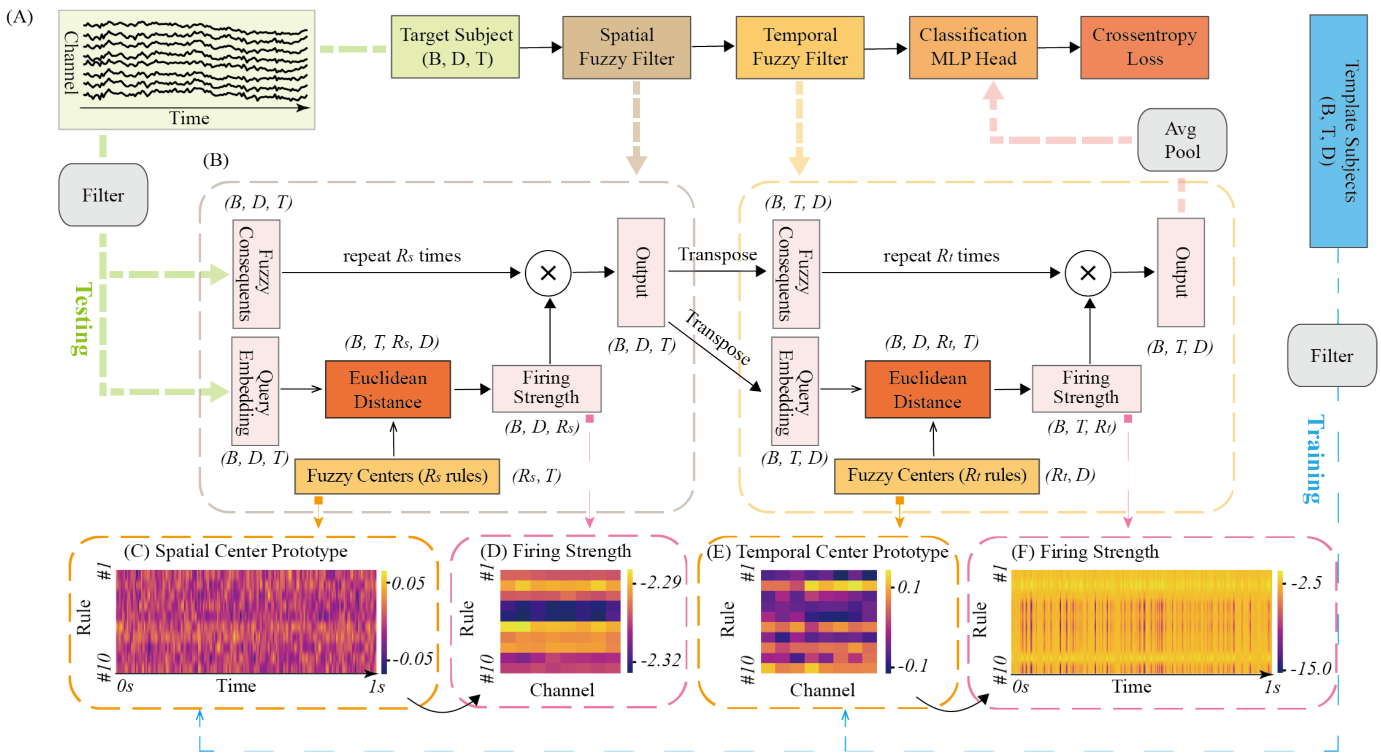

Fig. 2: Illustration of the architecture for predicting target frequencies in an SSVEP task using the proposed iFuzzyTL model. **(A)** Main structure of the iFuzzyTL model, where B represents the batch size, D denotes the number of feature dimensions, and T indicates the number of time points. **(B)** Design of the spatial and temporal fuzzy filters, where R_s and R_t denote the total number of rules for the spatial and temporal fuzzy filters, respectively. **(C)** Detected center using the spatial fuzzy filter. **(D)** Firing strength of a demonstration sample to show the learned neural pattern as identified by the spatial fuzzy filter. **(E)** Detected center using the temporal fuzzy filter. **(F)** Firing strength of a demonstration sample to show the learned neural pattern as identified by the temporal fuzzy filter.

where x_i denotes the input variables, D represents the number of feature dimensions, R denotes the total number of rules, u_r is the consequent of the r^{th} rule, and $A_{i,r}$ are the fuzzy sets corresponding to the r^{th} rule for i^{th} sample. Each fuzzy set $A_{i,r}$ is defined by the membership functions $A_{i,r}(x_i)$, where i ranges from 1 to D.

The firing strength α_r for rule r, which quantifies the degree to which the rule's conditions are satisfied and directly influence the rule's impact on the model's output, is computed as the product of the membership values for all input variables:

$$\alpha_r(x) = \prod_{i=1}^{D} A_{i,r}(x_i), \tag{5}$$

To facilitate a probabilistic interpretation of the outputs, the TSK FIS normalizes the firing strength α_r as $\overline{f_r}$, treating the normalized values as a probability distribution:

$$\overline{f_r}(x) = \frac{\alpha_r(x)}{\sum_{i=1}^{R} \alpha_i(x)} \tag{6}$$

where R is the number of rules.

The aggregated output y of the TSK FIS is then computed using a weighted average of the rule outputs:

$$y = \sum_{j=1}^{R} \frac{\alpha_j(x) u_j}{\sum_{i=1}^{R} \alpha_i(x)}, \tag{7}$$

In our study, Gaussian membership functions were chosen following the neuroscience study [46], due to the ability to accurately represent the normally distributed nature of biological and neural data observed in neuroscience:

$$\alpha_r(x) = \prod_{d=1}^{D} \exp\left(-\frac{(x_d - m_{r,d})^2}{2\sigma_{r,d}^2}\right) \tag{8}$$

$$= \exp\left(-\sum_{d=1}^{D} \frac{(x_d - m_{r,d})^2}{2\sigma_{r,d}^2}\right) \tag{9}$$

Here, r indexes the fuzzy rules, $m_{r,d}$ and $\sigma_{r,d}$ denote the centers and widths of the Gaussian fuzzy sets for the feature dimension d of each rule r, respectively. Both parameters $m_{r,d}$ and $\sigma_{r,d}$ are learnable and are optimized during training.

The normalized firing strength $\overline{f_r}(x)$ can be then simplified to:

$$\begin{aligned}\overline{f_r}(x) &= \frac{\alpha_r(x)}{\sum_{i=1}^{R} \alpha_i(x)} \\ &= \frac{\exp\left(-\sum_{d=1}^{D} \frac{(x_d - m_{r,d})^2}{2\sigma_{r,d}^2}\right)}{\sum_{i=1}^{R} \exp\left(-\sum_{d=1}^{D} \frac{(x_d - m_{i,d})^2}{2\sigma_{i,d}^2}\right)} \\ &= \text{softmax}\left(-\sum_{d=1}^{D} \frac{(x_d - m_{r,d})^2}{2\sigma_{r,d}^2}\right)\end{aligned} \tag{10}$$

Incorporated within this framework is an attention mechanism that enhances the interpretability and effectiveness of the FIS [46]. This mechanism is formally defined by the following equation:

$$Attention(x) = \text{softmax}(f(x)) \cdot g(x), \tag{11}$$

where $f(x)$ denotes the mapping from inputs to attention scores within the TSK FIS, specifically corresponding to the normalized firing strength $\overline{f_r}(x)$. The function $g(x)$ represents the transformation applied to the inputs, which modulates the influence of each input based on the computed attention scores. Here, $g(x)$ effectively utilizes the consequents u_r associated with each rule, thereby influencing the output based on the degree of relevance as determined by the attention mechanism.

2) Fuzzy Attention Layer as an Adaptive Spatial Filter in Signal Processing: Consider an input signal $x(t)$ processed through an adaptive filter. The output $Y(t)$ at time t is modeled as an adaptive linear combiner (ALC):

$$Y(t) = {W_S}^T \cdot x(t) \tag{12}$$

where $x(t)$ denotes the input feature vector at time t, and W_S represents the adaptive weights for all channels as a spatial filter.

By incorporating this fuzzy attention mechanism, we assign the adaptive weights as ${W_S}^T = \overline{f_r}(x(t))$, following the eq. (7) for each rule r and the filter's output $Y_S(t)$ becomes:

$$Y_S(t) = \sum_{r=1}^{R} \overline{f_r}(W_r^Q x(t)) \cdot W_r^V x(t) \tag{13}$$

where the projections are parameter matrices W_r^V and W_r^Q for rule r. This formulation enables the filter to adaptively modulate the importance of different features of $x(t)$ based on their alignment with the fuzzy rule centers. The fuzzy attention mechanism dynamically adjusts the attention weights in response to the proximity of the input features to the fuzzy set centers, effectively allowing the filter to highlight or suppress certain signal features according to their fuzzy membership values.

3) Fuzzy Attention as an Adaptive Temporal Filter: Here, fuzzy attention also functions as a temporal filter. The output Y for each channel c is given by:

$$Y(c) = {W_T}^T x(c) \tag{14}$$

where $x(c)$ represents the input feature matrix for channel c, and W_T is the adaptive weight vector. This vector modulates the attention mechanism in the time domain, corresponding to each channel c.

Thus, the temporal filter's output becomes:

$$Y_T(c) = \sum_{r=1}^{R} \overline{f_r}(W_r^Q x(c)) \cdot W_r^V x(c) \tag{15}$$

where the projections are parameter matrices W_r^V and W_r^Q corresponding to rule r. This configuration allows the Fuzzy Attention Layer to adaptively weigh time points based on their proximity to the fuzzy rule centers. This enhances the filter's ability to selectively focus on the most relevant temporal features for each channel c, thus improving the signal's interpretability and the overall accuracy of the analysis.

4) Input Recovery in Single-Layer Linear Networks: This section demonstrates that the original input of a single-layer linear transformation, referred to as a projector, can be reconstructed from its output, termed the query. This recovery is contingent on the condition that the transformation matrix W is non-singular. The invertibility of W thus ensures the feasibility of interpretability within the iFuzzyTL framework.

Consider the linear transformation defined by:

$$y = Wx + b \tag{16}$$

where y represents the output query, x the original input, W the transformation matrix, and b the bias vector.

To retrieve x from y, rearrange the above equation to:

$$Wx = y - b \tag{17}$$

Given W is non-singular, the inversion of W is feasible, allowing for the calculation of x by:

$$x = W^{-1}(y - b) \tag{18}$$

This illustrates that the original input x is retrievable directly from the output y when W is invertible.

For scenarios where W is singular or not a square matrix, the recovery of x employs the Moore-Penrose pseudoinverse W^+:

$$x = W^+(y - b) \tag{19}$$

The computation of W^+ utilizes the Singular Value Decomposition (SVD) of W:

$$W = U\Sigma V^T \tag{20}$$

where U and V are orthogonal matrices, and Σ contains the singular values.

The pseudoinverse W^+ is then:

$$W^+ = V\Sigma^+ U^T \tag{21}$$

with Σ^+ derived by inverting the non-zero singular values of Σ and taking the transpose.

This approach guarantees that if the dimensions of the input data and the output query match, the reconstructed input will correspond to the original input.

In conclusion, under the condition that W is either invertible or suitably approximated via its pseudoinverse, the reversibility of the input from the output in a single-layer linear model is effectively demonstrated.

5) Fuzzy Attention for SSVEP Transfer Learning: Our proposed model, iFuzzyTL, integrates three key components tailored for SSVEP signal processing: the spatial fuzzy filter, the temporal fuzzy filter, and the classification head. Both fuzzy filters follow the design as the adaptive filers in eqs. (13) and (15).

The model architecture is depicted in Fig. 2(A). The spatial fuzzy filter initially processes the data, considering channel-like centers (R_s, C), followed by a transpose operation. Subsequently, the temporal fuzzy filter applies, which adapts to signal-like centers (R_t, S), where R_s and R_t denote the total number of rules for the spatial and temporal fuzzy filters, respectively. This dual filtering strategy enables the model to encode both spatial and temporal dimensions of the SSVEP signals effectively. The structure of the spatial and temporal fuzzy filters are shown in Fig. 2(B).

The classification head consists of a 2-layer Multi-Layer Perceptron (MLP) model with ReLU (Rectified Linear Unit) activation and a dropout rate of 0.3 during training. The number of output nodes in the classification head corresponds to the number of labels.

The primary goal is to classify the SSVEP target frequencies accurately. We employ a multiclass cross-entropy loss function for this purpose, defined as:

$$\text{loss}(y_{o,c}, p_{o,c}) = -\sum_{c=1}^{M} y_{o,c} \log(p_{o,c}) \tag{22}$$

Where $y_{o,c}$ denotes the true label, $p_{o,c}$ represents the predicted probability for class c, and M is the total number of classes or target frequencies in the classification schema. This loss function quantifies the discrepancy between predicted probabilities and the actual class labels, facilitating practical model training to recognize SSVEP frequencies.

D. Evaluation Metrics

To evaluate the performance of each method, we used two primary metrics: classification accuracy and ITR. Classification accuracy is defined as the ratio of correctly classified samples to the total number of test samples.

The ITR, measured in bits per minute (bits/min), quantifies the speed and accuracy of a brain-computer interface and is computed as follows [74]:

$$\text{ITR} = \frac{60}{T + T_{run}} [\log_2 N + P \log_2 P + (1-P) \log_2 \frac{1-P}{N-1}] \tag{23}$$

where T is the average time required for each selection operation, T_{run} is the running time, N represents the number of possible classes, and P is the classification accuracy. Following previous studies [15, 69], an additional 0.5 s was included in T to account for gaze shift time. For example, if the data length is 1 s, T is set to 1.5 s for the ITR calculation using the formula above.

In this study, we focused on zero-shot inter-subject classification experiments. We employed the leave-one-out cross-validation method, where the data from one subject was used as the test set while the data from all other subjects formed the training set, as shown in Fig. 1(C) and 2(A). This process was repeated until each subject had been used as the test subject once, ensuring a complete evaluation.

The baseline model and dataset description are in Supplementary Sections 1.1 and 1.2, respectively.

III. Results

The average classification accuracies and ITR of the seven methods on the 12JFPM dataset are presented in Table I and Supplementary Table I, respectively. Data lengths range from 0.5 s to 1.2 s in 0.1 s intervals, with additional lengths of 1.5 s and 2 s included to evaluate model performance over extended durations. The results indicate that iFuzzyTL consistently outperforms other baseline methods, achieving the highest average classification accuracies and ITR for data lengths under 1.1 s. However, for lengths of 1.2s, 1.5 s and 2 s, FB-SSVEPformer demonstrated superior performance compared to iFuzzyTL.

For classification accuracies, a two-way repeated measures ANOVA (rm-ANOVA) revealed significant main effects of data length ($F(9, 81) = 244.49$, $p < 0.001$) and method ($F(7, 63) = 7.17$, $p < 0.001$), as well as a significant interaction effect between them ($F(63, 567) = 15.39$, $p < 0.001$). Paired t-tests were conducted at each data length to compare iFuzzyTL with baseline methods, with statistical results summarized in Table I. iFuzzyTL showed significant improvements over all methods for data lengths ranging from 0.5 s to 1.1 s. when the data lengths are longer than 1.2 s, the accuracy of FB-SSVEPformer is higher than that of iFuzzyTL ($p > 0.05$). Regarding ITR, the rm-ANOVA also indicated significant main effects of data length ($F(9, 81) = 13.86$, $p < 0.001$) and method ($F(63) = 7.01$, $p < 0.001$), along with a significant interaction effect between them ($F(63, 567) = 6.76$, $p < 0.001$). The detailed statistical results by paired t-tests are presented in Supplementary Table I. The results revealed that iFuzzyTL outperformed all baseline methods.

The average classification accuracies and ITR for the seven methods on the eldBETA dataset are shown in Table II and Supplementary Table II, respectively. Data lengths span from 0.5 s to 1.2 s in 0.1 s intervals, with additional evaluations at 1.5 s and 2 s. The two-way rm-ANOVA for classification accuracies revealed significant main effects of data length ($F(9, 891) = 530.76$, $p < 0.001$) and method ($F(7, 693) = 29.28$, $p < 0.001$), with a significant interaction effect ($F(63, 6237) = 18.32$, $p < 0.001$). Paired t-tests further indicated significant differences between iFuzzyTL and other methods, except some data lengths of CCNN. SSVEPformer, and FB-SSVEPformer. Particularly, iFuzzyTL significantly outperformed CCNN at 0.5 s, 0.7 s, 1.1 s, 1.5 s, and 2.0 s ($p < 0.05$) and FB-SSVEPformer at 0.7 s ($p < 0.05$). For ITR, significant main effects of data length ($F(9, 891) = 72.93$, $p < 0.001$) and method ($F(7, 693) = 31.71$, $p < 0.001$), as well as a significant interaction effect ($F(63, 6237) = 29.80$, $p < 0.001$) were found. The detailed statistical results by paired t-tests are presented in Supplementary Table II. the ITR of iFuzzyTL is higher than others at 1.5 s and 2.0 s ($p < 0.05$).

The average classification accuracies and ITR on the Benchmark dataset are reported in Table **??** and Supplementary Table III, respectively. Data lengths range from 0.5 s to 1.2 s, with additional evaluations at 1.5 s and 2 s. For classification accuracies, the two-way rm-ANOVA showed significant main effects of data length ($F(9, 306) = 550.93$, $p < 0.001$) and method ($F(238) = 16.55$, $p < 0.001$), and a significant interaction effect ($F(63, 2142) = 20.29$, $p < 0.001$). Paired t-tests indicated significant differences between iFuzzyTL and TRCA, eCCA, EEGNET, SCCA_qr ($p < 0.001$). As for CCNN, the accuracy of iFuzzyTL is higher at the data length longer than 0.8s ($p < 0.05$). There is no significant difference among iFuzzyTL, SSVEPformer, and FB-SSVEPformer ($p > 0.05$) of accuracy. Regarding ITR, significant main effects of data length ($F(9, 306) = 46.20$, $p < 0.001$) and method ($F(7, 238) = 25.60$, $p < 0.001$), as well as a significant interaction effect ($F(63, 2142) = 22.81$, $p < 0.001$), were observed. Paired t-tests indicated significant differences between iFuzzyTL and TRCA, eCCA, EEGNET, SCCA_qr ($p < 0.001$). the ITR of iFuzzyTL is higher than CCNN ($p < 0.05$) except at 0.6 s, 0.7 s, and 0.8 s ($p > 0.05$). There is no significant difference among iFuzzyTL, SSVEPformer, and FB-SSVEPformer ($p > 0.05$) of ITR.

Our method exhibited a gradual decline in performance across three datasets as the input length decreased. From a signal processing perspective, shorter window lengths result in a reduced number of periodic components, leading to inadequate frequency resolution that affect the recognition of target frequencies [75, 76]. For model training, the limited frequency information contained in shorter data sequences results in a diminished quality of the training dataset. During the training process, the model may rely on features which are unrelated to SSVEP, resulting in overfitting and a subsequent decrease in validation set accuracy.

IV. Real-Time Feasibility Evaluation

To evaluate the feasibility of the proposed model in real-world applications, we conducted an online experiment consisting of a data collection session and an online test session. The descriptions of Experiment Design, Participants and Data Acquisition, Procedure for Training Data Collection, and Data Preprocessing are presented in Supplementary Material Section II.

During the online testing phase, we adopted a 'leave-one-out' cross-validation strategy for evaluation. Specifically, the model was trained using data from five out of six trained subjects, with the remaining subject's data reserved for testing. This pre-trained model was then incorporated into our online BCI system.

Each online trial commenced with the presentation of a cue, directing the subject to focus on a designated flashing flicker. The onset of the flicker was marked by a 'start' signal sent to the system terminal via UDP, initiating the recording of task-related EEG data. Upon completion of the flicker sequence, lasting 1.5 seconds, an 'end' marker was transmitted, signaling the cessation of data recording and the start of data segmentation. Considering that spontaneous EEG signals in the initial phase may introduce noise and variability [69], our model utilized EEG data from the 0.5 to 1.5 second interval for input.

Each subject participated in three rounds of the experiment, yielding a total of 36 trials per subject. The performance evaluation of our model was based on the accuracy and ITR recorded during these 1-second real-time experiments. Additionally, any trials experiencing dropped frames in the AR interface were excluded from the analysis to maintain the integrity and consistency of the dataset.

The results demonstrated a high level of effectiveness, with an average accuracy of $90.13\% \pm 2.27\%$, and an ITR of 164.93 ± 9.11 bits/min. After this, the baseline performances are tested based on the recorded data. Notably, the accuracy achieved by our model significantly surpassed that of TRCA, EEGNet, SCCA_qr, and SSVEPformer ($p < 0.05$), as shown in Fig. 4.

V. Discussion

In the iFuzzyTL framework, the *center* plays a key role by encapsulating domain knowledge derived from source domains. It acts as a general *template*, effectively capturing the essence of the source domain characteristics. By computing the distance between this learned center and incoming data points, the model robustly leverages the underlying domain knowledge to make informed decisions. This mechanism facilitates robust decision-making and significantly enhances the model's transferability across different SSVEP tasks. Incorporating the center as a template proves advantageous for SSVEP applications, where the ability to generalize across varying conditions and subjects is crucial. Consequently, iFuzzyTL offers an improved approach to handling the inherent variability in SSVEP signals, ensuring higher performance and reliability in real-world scenarios.

A. Sample-wised Interpretability Analysis

1) Demo Analysis of SSVEP Target Frequency Identification Using iFuzzyTL Model: To provide an intuitive understanding of how the iFuzzyTL model identifies the SSVEP target frequency, we present a demo sample from the best-performing subject (S8) in the 12JFPM dataset, with a target frequency of 9.25 Hz, as shown in Fig. 2(A). Fig. 2(C) illustrates that the spatial fuzzy filter's center pattern resembles the EEG signal, with distinct phases for each rule. In Fig. 2(D), the border firing strength indicates that the contributions of rules #4 and #5 for this sample are minimal, while channels 1 and 2 contribute significantly to rule #6.

After applying the spatial filter, Fig. 2(E) demonstrates the center of the temporal fuzzy filter for subject S8, displaying the neural patterns captured across 10 separate rules. Particularly, rule #2 shows a high contribution in most channels, whereas rules #1 and #5 exhibit the lowest contribution. Additionally, Fig. 2(F) reveals that the firing strength in the temporal fuzzy filter indicates a stable pattern for rules #4-8 and #10 in this sample.

2) Analysis of Temporal Firing Strength Features in the Frequency Domain: To further investigate how the fuzzy rules learns features in the time domain, we compute the FFT of the input feature that triggered the fuzzy rules in the proposed temporal filter. The results indicate that the firing strength exhibits peaks at harmonic frequencies in correct case, as demonstrated in Fig. 5.

In the left panel, corresponding to a target frequency of 9.25 Hz, a prominent peak is observed at 28 Hz. This shift is attributed to the relatively low sample rate, which causes the harmonic frequencies in the FFT to exhibit slight displacements. The middle panel illustrates a target frequency of 10.25 Hz, with peaks observed at both 10.5 Hz and 41.5 Hz. In contrast, the right panel presents a less favorable case with a target frequency of 13.25 Hz, where peaks near 27 Hz are detected across several rules, indicating that not all rules accurately capture the target frequency, although some rules remain effective.

TABLE I: Average accuracies (%) across subjects for six methods at different data lengths on Dataset 12JFPM. Asterisks indicate significant differences between iFuzzyTL and the other methods, as assessed by paired t-tests (*$p < 0.05$, **$p < 0.01$, ***$p < 0.001$). The percentages in brackets is standard deviation.

Model	0.5s	0.6s	0.7s	0.8s	0.9s	1.0s	1.1s	1.2s	1.5s	2.0s
TRCA	18.33% (6.32%) ***	22.94% (9.16%) ***	30.89% (12.52%) ***	36.61% (15.98%) ***	45.67% (18.27%) ***	52.94% (22.06%) ***	57.61% (22.83%) ***	62.11% (24.00%) ***	74.39% (23.63%) **	84.39% (19.72%) *
eCCA	54.94% (21.86%) *	61.11% (25.97%) *	64.39% (27.22%) **	67.78% (28.34%) *	73.11% (27.47%) *	75.56% (26.35%) *	77.44% (26.92%) *	79.78% (24.80%) *	85.28% (21.88%)	88.06% (20.34%)
CCNN	64.61% (22.29%)	66.56% (23.43%) ***	72.33% (23.23%) *	77.36% (15.20%) ***	82.50% (18.60%)	84.00% (18.09%)	86.11% (14.72%) ***	88.83% (13.54%)	92.39% (10.46%)	95.44% (7.86%)
EEGNET	50.11% (17.58%) **	56.00% (23.12%) **	62.94% (21.36%) ***	66.44% (23.31%) ***	70.28% (23.60%) **	75.11% (22.46%) **	77.61% (21.88%) *	79.72% (22.35%) *	87.28% (15.46%)	90.44% (13.17%)
SCCA_qr	54.83% (21.93%) *	61.44% (24.54%) *	66.89% (26.25%) **	72.39% (27.99%) *	76.44% (27.26%) *	78.83% (25.84%) *	81.72% (25.07%)	84.17% (22.66%)	88.78% (16.72%)	93.44% (12.85%)
SSVEPformer	66.22% (22.40%)	68.67% (22.12%)	75.22% (21.91%)	78.67% (21.58%)	82.11% (19.61%)	84.06% (18.17%)	86.06% (16.79%)	88.56% (14.32%)	92.61% (11.08%)	95.00% (8.36%)
FB-SSVEPformer	65.83% (22.98%)	72.39% (22.90%)	77.44% (21.49%)	82.17% (20.30%)	85.83% (18.87%)	87.61% (17.45%)	89.39% (15.99%)	**91.28% (13.85%)**	**94.78% (9.82%)**	**96.00% (9.12%)**
iFuzzyTL	**67.92% (12.59%)**	**75.29% (15.28%)**	**81.91% (16.42%)**	**84.76% (15.36%)**	**88.64% (16.10%)**	**89.70% (14.89%)**	**90.22% (13.99%)**	90.14% (13.88%)	91.97% (15.42%)	92.41% (14.26%)

Note: Entries in bold indicate the model with the best performance.

TABLE II: Average accuracies (%) across subjects for six methods at different data lengths on Dataset eldBETA. Asterisks indicate significant differences between iFuzzyTL and the other methods, as assessed by paired t-tests (*$p < 0.05$, **$p < 0.01$, ***$p < 0.001$). The percentages in brackets is standard deviation.

Model	0.5s	0.6s	0.7s	0.8s	0.9s	1.0s	1.1s	1.2s	1.5s	2.0s
TRCA	42.05% (19.30%) ***	44.17% (20.15%) ***	45.75% (20.98%) ***	48.40% (21.45%) ***	51.14% (22.69%) ***	52.54% (23.20%) ***	55.17% (23.26%) ***	56.51% (23.68%) ***	60.48% (24.23%) ***	61.86% (24.63%) ***
eCCA	46.60% (19.35%) ***	51.16% (20.26%) ***	55.52% (21.57%) ***	58.73% (22.32%) ***	62.60% (22.47%) ***	65.54% (22.62%) ***	68.16% (22.32%) ***	70.54% (21.74%) ***	75.30% (20.66%) ***	80.14% (19.25%) ***
CCNN	62.29% (21.09%) **	65.05% (21.14%)	68.63% (21.52%) ***	70.90% (21.52%)	73.05% (21.62%)	74.95% (21.04%)	76.30% (20.70%) **	77.63% (20.47%)	81.14% (19.04%) **	83.98% (17.97%) **
EEGNET	57.51% (21.14%) ***	59.46% (22.38%) ***	62.00% (23.06%) ***	64.37% (22.63%) ***	65.97% (23.22%) ***	67.25% (23.43%) ***	68.65% (23.20%) ***	69.24% (23.76%) ***	71.76% (23.29%) ***	74.13% (22.87%) ***
SCCA_qr	41.70% (19.48%) ***	49.22% (21.13%) ***	53.84% (22.04%) ***	57.92% (22.37%) ***	61.38% (22.69%) ***	64.75% (22.68%) ***	67.35% (22.56%) ***	69.30% (22.63%) ***	74.62% (21.52%) ***	81.00% (18.90%) ***
SSVEPformer	62.73% (23.12%)	65.71% (23.18%)	69.49% (22.72%)	71.25% (22.62%)	73.48% (22.60%)	75.41% (21.89%)	76.79% (21.08%)	77.84% (21.69%)	81.33% (19.85%)	83.97% (18.31%)
FB-SSVEPformer	61.14% (23.97%)	64.27% (23.75%)	67.13% (23.79%) *	69.89% (23.55%)	72.43% (23.07%)	73.97% (22.72%)	75.54% (22.21%)	76.98% (22.13%)	80.14% (20.94%)	83.30% (19.67%)
iFuzzyTL	**66.48% (15.09%)**	**66.85% (15.46%)**	**74.02% (16.91%)**	**71.45% (17.40%)**	**74.00% (17.54%)**	**76.50% (17.19%)**	**80.17% (17.34%)**	**78.82% (18.05%)**	**84.16% (16.35%)**	**86.70% (15.67%)**

Note: Entries in bold indicate the model with the best performance.

TABLE III: Average accuracies (%) across subjects for six methods at different data lengths on Dataset Benchmark. Asterisks indicate significant differences between iFuzzyTL and the other methods, as assessed by paired t-tests (*$p < 0.05$, **$p < 0.01$, ***$p < 0.001$). The percentages in brackets is standard deviation.

Model	0.5s	0.6s	0.7s	0.8s	0.9s	1.0s	1.1s	1.2s	1.5s	2.0s
TRCA	42.05% (19.30%) ***	44.17% (20.15%) ***	45.75% (20.98%) ***	48.40% (21.45%) ***	51.14% (22.69%) ***	52.54% (23.20%) ***	55.17% (23.26%) ***	56.51% (23.68%) ***	60.48% (24.23%) ***	61.86% (24.63%) ***
eCCA	46.60% (19.35%) ***	51.16% (20.26%) ***	55.52% (21.57%) ***	58.73% (22.32%) ***	62.60% (22.47%) ***	65.54% (22.62%) ***	68.16% (22.32%) ***	70.54% (21.74%) ***	75.30% (20.66%) ***	80.14% (19.25%) ***
CCNN	62.29% (21.09%) **	65.05% (21.14%)	68.63% (21.52%) ***	70.90% (21.52%)	73.05% (21.62%)	74.95% (21.04%)	76.30% (20.70%) **	77.63% (20.47%)	81.14% (19.04%) **	83.98% (17.97%) **
EEGNET	57.51% (21.14%) ***	59.46% (22.38%) ***	62.00% (23.06%) ***	64.37% (22.63%) ***	65.97% (23.22%) ***	67.25% (23.43%) ***	68.65% (23.20%) ***	69.24% (23.76%) ***	71.76% (23.29%) ***	74.13% (22.87%) ***
SCCA_qr	41.70% (19.48%) ***	49.22% (21.13%) ***	53.84% (22.04%) ***	57.92% (22.37%) ***	61.38% (22.69%) ***	64.75% (22.68%) ***	67.35% (22.56%) ***	69.30% (22.63%) ***	74.62% (21.52%) ***	81.00% (18.90%) ***
SSVEPformer	62.73% (23.12%)	65.71% (23.18%)	69.49% (22.72%)	71.25% (22.62%)	73.48% (22.60%)	75.41% (21.89%)	76.79% (21.08%)	77.84% (21.69%)	81.33% (19.85%)	83.97% (18.31%)
FB-SSVEPformer	61.14% (23.97%)	64.27% (23.75%)	67.13% (23.79%) *	69.89% (23.55%)	72.43% (23.07%)	73.97% (22.72%)	75.54% (22.21%)	76.98% (22.13%)	80.14% (20.94%)	83.30% (19.67%)
iFuzzyTL	**66.48% (15.09%)**	**66.85% (15.46%)**	**74.02% (16.91%)**	**71.45% (17.40%)**	**74.00% (17.54%)**	**76.50% (17.19%)**	**80.17% (17.34%)**	**78.82% (18.05%)**	**84.16% (16.35%)**	**86.70% (15.67%)**

Note: Entries in bold indicate the model with the best performance.

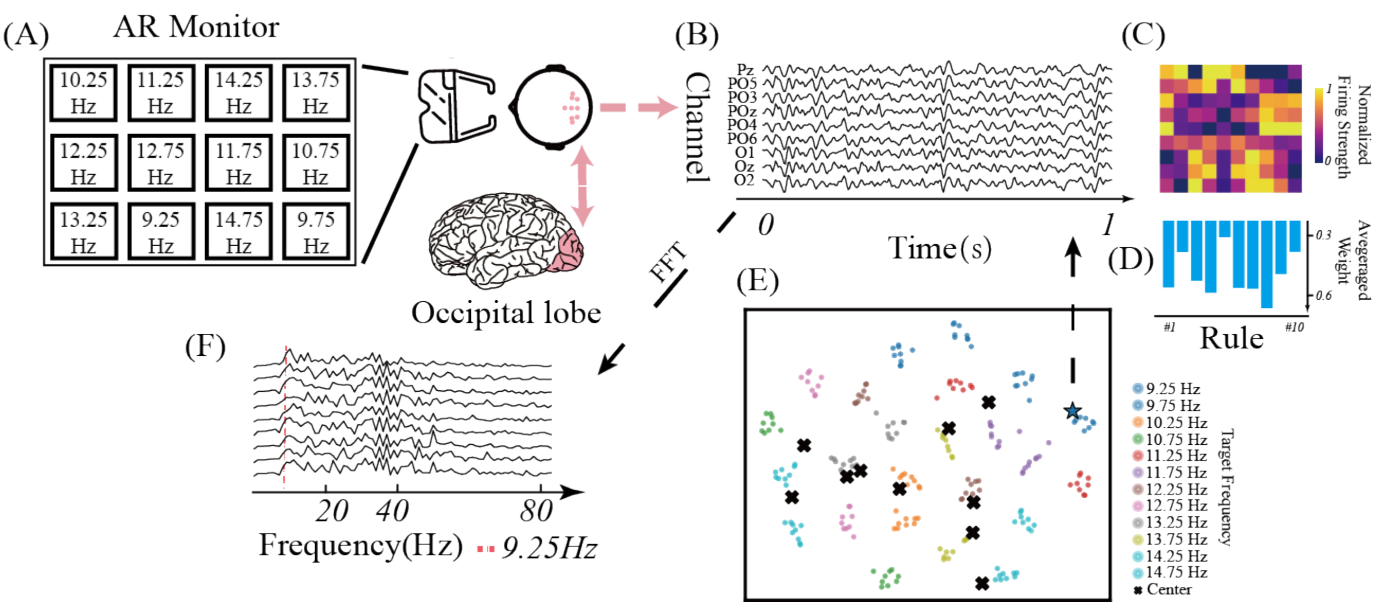

Fig. 3: Detailed illustration of a real-time SSVEP experiment setup. **(A)** Demonstration setup for the experiment. The EEG channels are located in the occipital lobe. **(B)** Example of a filtered EEG signal used in the demo. **(C)** Min-max normalized firing strength across the rules. **(D)** Averaged weight distribution among the rules (without normalization). **(E)** Data distribution following the application of the spatial filter. **(F)** Fourier Transform results of the demo EEG signal.

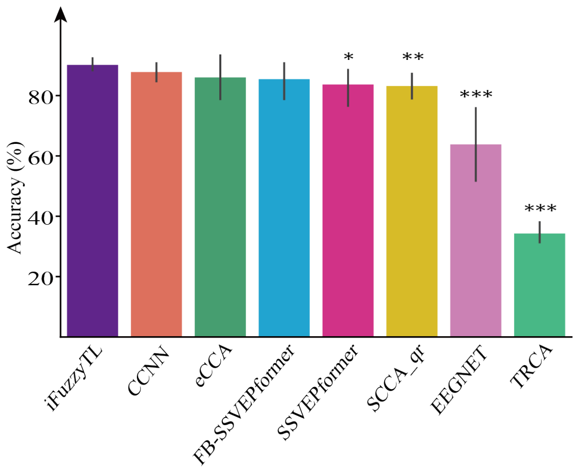

Fig. 4: Comparison of the model with other SOTA models in the online experiment. The significant differences between iFuzzyTL model and other models are highlighted by paired t-tests ($*p < 0.05$, $**p < 0.01$, $***p < 0.001$).

B. Deeper Analysis of Correct and Incorrect Cases

For deeper understanding of correct and incorrect cases of iFuzzyTL model, we randomly select one sample from the same target frequency (11.75 Hz) from three subjects (S2, S6, and S8) who exhibited varying performance levels (input data length as 1s: S2: 55.12%, S6: 96.95%, S8: 99.17%; input data length as 2s: S2: 55.12%, S6: 100%, S8: 100%). Subject S8 demonstrated the best performance among all subjects in the 12JFPM dataset across all tested models, while subject S6 performed better than subject S2 but worse than subject S8. Subject S2 showed the worst performance across all models. Then, we compare how the iFuzzyTL model processes the EEG signal in three different-quality subjects.

As shown in Fig. 6(A), the data distribution after applying the spatial filter for subject S8 is highly clustered and distinct, whereas subject S6 shows a less distinct clustering pattern and subject S2 exhibits the weakest clustering. For subject S8, the fuzzy centers are mostly located within the clusters corresponding to each target frequency, whereas for subjects S6 and S2, the center alignment is less clear.

In Fig. 6(C), The firing strength of the spatial fuzzy filter for the selected sample of subject S8 is more consistent across the rules, with Channels 6 and 7 significantly contributing to the decision-making process. As for subject S6, the contributions vary more across different rules, with Channels 7 and 8 being important overall, while Channels 2, 3, and 5 play key roles in specific rules (#4, #1&2, and #6&10, respectively). In contrast, the firing strength of subject S2 has an unclear pattern. Channels 4-8 show major contributions across different rules.

To better understand these differences, we refer to Fig. 6(B). It is well-known that FFT features are crucial for SSVEP. In subject S8, the signal quality across all channels in this sample is high, enabling the spatial filter to effectively select the optimal channels for adaptive filtering, thereby enhancing model prediction accuracy. As for subject S6, the channel quality is moderate, as evidenced by multiple peaks in the FFT, which include both target and harmonic frequencies. Consequently, the filter relies on information from more channels to achieve satisfactory results and eventually make correct predictions. Conversely, subject S2 exhibits poor overall channel quality, with detectable peaks in Channels 6, 7, 8, 9, and 10 in the FFT though the peak is not clear. However, Channels 1, 2, and 3 display multiple unclear frequency peaks. This causes the spatial filter to apply different rules when selecting these channels. Thus, distinctive rules are created in a fragmented manner, and incorrect predictions are made in subject S2.

Similarly, in our real-time test, as shown in Figs. 3(B) (raw signal) and 3(F) (FFT result), the FFT peaks of Channels Pz and PO5 are prominent, and their contribution in Rule #4 is substantial. The data distribution for this scenario is also as clear as that of subject S8 in the 12JFPM dataset, as illustrated in Fig. 3(E). Particularly, during the application of the spatial filter, the fuzzy attention mechanism may not strictly filter channels. For example, as shown in Fig. 3(D), Rule #8 has the highest average weight, yet it selects Channels PO3, POz, and PO4, which are not strongly indicated by FFT. This discrepancy may be attributed to the limited diversity of the small training set.

In summary, these findings suggest that iFuzzyTL can better learn the knowledge from the source domain and predict the result if the signal is clear; otherwise, iFuzzyTL can effectively select high-quality channels by the spatial filter through a combination of rules, thus enhancing the filtering of input signals, but may cause the incorrect predictions.

C. Ablation Study

The ablation study was meticulously designed to rigorously evaluate the influence of various parameters and modules of our proposed Fuzzy rule-based framework, iFuzzyTL, on its performance. This systematic examination helps uncover the contributions of individual components and configurations to the overall efficacy and operational dynamics of the model. All statistical comparisons were conducted using paired t-tests to assess the significance of differences.

1) Filter Effect Analysis: In this study, we assessed the performance impact of various configurations and types of fuzzy filters on signal processing. The primary motivation was to elucidate the relative importance of spatial versus temporal filtering and to determine the influence of their application sequence on the quality of the resultant data. The significance test and result are shown in Fig. 7.

a) Impact of Filter Application Order: Our experimental setup tested two different sequences of applying filters to ascertain their influence on signal integrity and feature isolation. The first sequence involved applying a spatial filter followed by a temporal filter aimed at reducing spatial noise to enhance signal clarity before isolating temporal features. The alternative sequence started with a temporal filter intended to highlight temporal dynamics, followed by a spatial filter to refine the signal's spatial characteristics. Notably, significant differences were observed predominantly in the eldBETA dataset ($p < 0.05$), where the spatial filter followed by the temporal filter

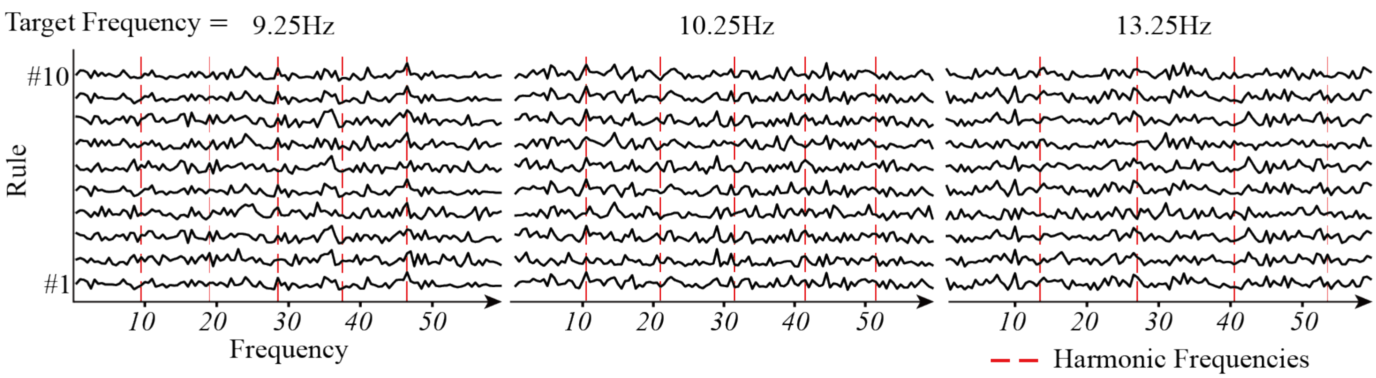

Fig. 5: FFT features that triggered each fuzzy rule across different target frequencies, illustrating the identification of harmonic peaks.

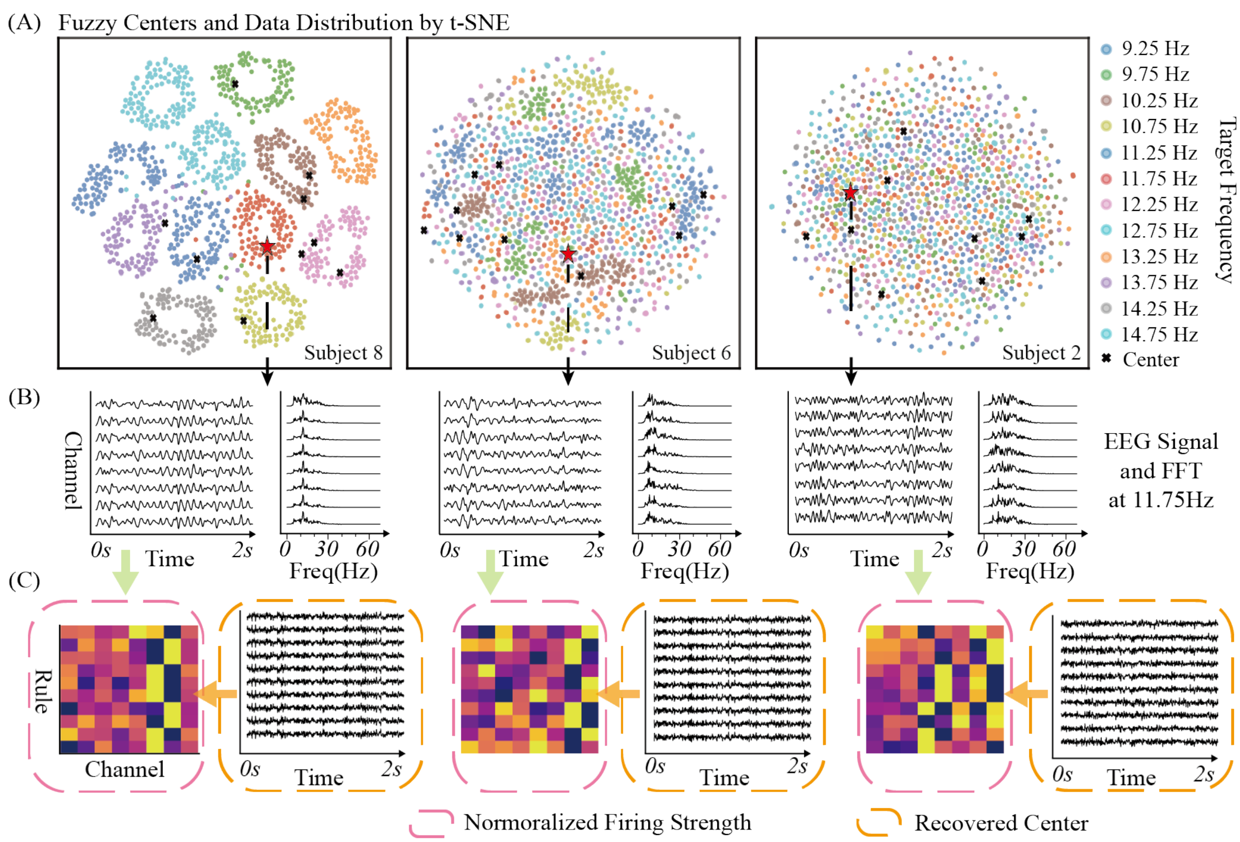

Fig. 6: Visualization of demographic subjects from the 12JFPM dataset (2s) illustrating what iFuzzyTL learned. **(A)** Data distribution post-application of the spatial filter, highlighting the position (Red Star) of a sample needing explanation at 11.75Hz. **(B)** Filtered EEG signals and their Fourier Transform to display the data characteristics. **(C)** Representation of firing strength and the center, using min-max normalization across the channel dimension to accentuate differences within one rule. The center is reconstructed from the query space to the raw EEG signal space as described in Section II-C4.

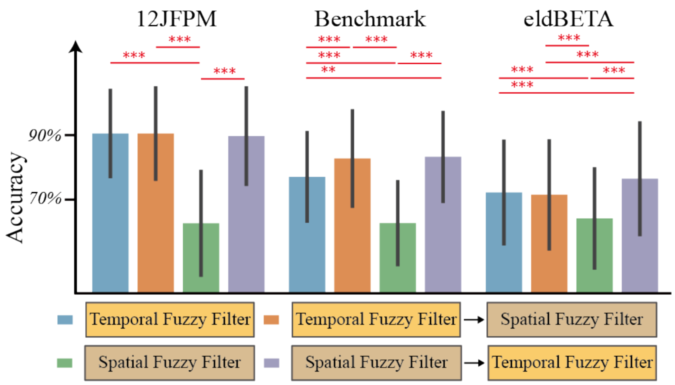

Fig. 7: Variation in accuracy as a function of different configurations of two fuzzy filter modules across three datasets. This figure illustrates the significant impact of filter type and sequence on model performance. $^{**}p < 0.01$, $^{***}p < 0.001$

sequence exhibited superior performance compared to the reverse sequence.

b) Evaluating Single Filter Types: The investigation also explored the effects of using each type of filter independently. The application of only a spatial filter was to evaluate the consequences of omitting temporal filtering, whereas using only a temporal filter was intended to assess whether spatial information alone could suffice for specific analytical tasks. The findings revealed that the exclusive use of a spatial filter significantly reduced performance across all datasets ($p < 0.05$). In contrast, employing only a temporal filter maintained relatively high performance, though it was slightly outperformed by the combined filter sequences in the Benchmark dataset.

After that, the comparison of the single filter with a combination of two filters is also tested. The results show that the bi-directional combination of two filters ($temporal filter \rightarrow spatial filter$ and reversed) is significantly better than the single spatial filter ($p < 0.05$) in three datasets. the Benchmark dataset shows a significant improvement from a single temporal filter to the bi-directional combination of two filters($p < 0.05$), and the eldBETA dataset shows a significant improvement from a single temporal filter to $spatial filter \rightarrow temporal filter$ combination of two filters ($p < 0.05$).

The results underscore the indispensable nature of the temporal filter, whereas the spatial filter, though beneficial, proved less critical. The sequence of filter application did not significantly impact performance, except in certain datasets where the spatial filter followed by temporal filter configuration slightly outperformed others. These findings contrast traditional approaches such as CCA, which primarily relies on spatial filtering. Moreover, recent methodologies that integrate temporal filters, such as TRCA and ECCA, further validate the relevance of our results [77]. To summarize, the proposed scheme employs spatial and temporal filters to significantly enhance interpretability by explicitly capturing neural activation patterns across both domains, thereby improving pattern recognition and facilitating transfer learning across subjects.

2) Number of Rule Effect Analysis: In this ablation study, which examines the impact of the number of rules within our model, Fig. 8 demonstrates the variability in accuracy across the 12JFPM, Benchmark, and eldBETA datasets with varying rule counts of 3, 5, 10, 15 and 20. Our results indicate that an increase from 3 to 10 rules generally enhances accuracy across all evaluated datasets ($p < 0.05$). Particularly, the Benchmark dataset shows the most significant enhancements when the rule count is increased from 3 to 5 and subsequently from 5 to 10, with all transitions showing statistical significance ($p < 0.05$). However, when rule counts are bigger than 10, there is no significant improvement ($p > 0.05$). This suggests that a moderate increase in model complexity can positively affect the model's transfer learning capabilities but not beyond a certain point. Meanwhile, the 12JFPM and eldBETA datasets display significant improvements predominantly for transitions from 5 to 10 and 3 to 10 ($p < 0.05$). Summarily, incorporating more rules extends the knowledge coverage, thereby increasing the capacity for domain adaptation, which is critical for effective transfer learning.

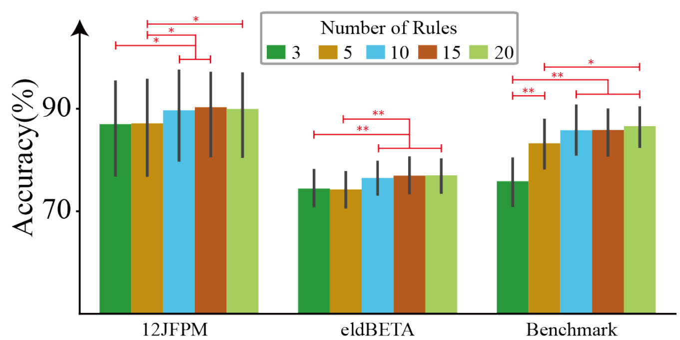

Fig. 8: Accuracy variation as a function of the number of rules across three datasets, highlighting the impact of rule number on model performance. $^{*}p < 0.05$, $^{**}p < 0.01$

VI. Limitations

Our study has identified several limitations with the iFuzzyTL model. Firstly, the model (rule count is 10) comprises approximately 400K parameters, which leads to longer training times, potentially limiting its efficiency in scenarios requiring quick deployment and can not automatically select the number of rules. Secondly, iFuzzyTL cannot be directly tested with a different set of devices if the electrode channel locations vary, as the model's performance is contingent on specific channel configurations. Lastly, the model does not support direct testing with different target frequencies without adjustments, which may restrict its application across diverse BCI setups where frequency variations are common.

VII. Future Work

Future work can further investigate methods to reduce the parameter count while maintaining or enhancing performance, automatically decide the number of rules, explore adaptable channel configuration strategies for greater device compatibility, and develop frequency-independent processing techniques to accommodate varying target frequencies such as regression model. To further enhance discrimination accuracy for short-duration SSVEP signals, initial efforts could focus on strengthening the preprocessing stage, such as introducing more features into the SSVEP paradigm or signal decomposition method. This will potentially broaden the applicability of iFuzzyTL across a wider range of BCI systems and real-world scenarios.

VIII. Conclusion

We propose iFuzzyTL, a fuzzy logic-based attention mechanism that enhances transfer learning in SSVEP BCI systems, significantly reducing user-specific calibration. By integrating fuzzy logic with neural networks, iFuzzyTL improves transferability and interpretability, crucial for zero-shot learning. Experiments confirm superior recognition accuracy in zero-calibration scenarios, outperforming real-time benchmarks. Its plug-and-play design enables deployment in dynamic environments without retraining, addressing key challenges in practical BCI applications. iFuzzyTL thus offers a high-performance, low-calibration solution for real-world SSVEP-based BCIs.

References

[1] N. Guo, X. Wang, D. Duanmu, X. Huang, X. Li, Y. Fan, H. Li, Y. Liu, E. H. K. Yeung, M. K. T. To *et al.*, "Ssvep-based brain computer interface controlled soft robotic glove for post-stroke hand function rehabilitation," *IEEE Transactions on Neural Systems and Rehabilitation Engineering*, vol. 30, pp. 1737–1744, 2022.

[2] X. Chen, X. Huang, Y. Wang, and X. Gao, "Combination of augmented reality based brain-computer interface and computer vision for high-level control of a robotic arm," *IEEE Transactions on Neural Systems and Rehabilitation Engineering*, vol. 28, no. 12, pp. 3140–3147, 2020.

[3] B. Cao, H. Niu, J. Hao, and G. Wang, "Building eeg-based cad object selection intention discrimination model using convolutional neural network (cnn)," *Advanced Engineering Informatics*, vol. 52, p. 101548, 2022.

[4] C.-T. Lin and T.-T. N. Do, "Direct-sense brain–computer interfaces and wearable computers," *IEEE Transactions on Systems, Man, and Cybernetics: Systems*, vol. 51, no. 1, pp. 298–312, 2020.

[5] S. Samejima, A. Khorasani, V. Ranganathan, J. Nakahara, N. M. Tolley, A. Boissenin, V. Shalchyan, M. R. Daliri, J. R. Smith, and C. T. Moritz, "Brain-computer-spinal interface restores upper limb function after spinal cord injury," *IEEE Transactions on Neural Systems and Rehabilitation Engineering*, vol. 29, pp. 1233–1242, 2021.

[6] M. Cheng, X. Gao, S. Gao, and D. Xu, "Design and implementation of a brain-computer interface with high transfer rates," *IEEE transactions on biomedical engineering*, vol. 49, no. 10, pp. 1181–1186, 2002.

[7] E. Yin, Z. Zhou, J. Jiang, Y. Yu, and D. Hu, "A dynamically optimized ssvep brain–computer interface (bci) speller," *IEEE Transactions on Biomedical Engineering*, vol. 62, no. 6, pp. 1447–1456, 2015.

[8] H. Cecotti and A. Graser, "Convolutional neural networks for p300 detection with application to brain-computer interfaces," *IEEE transactions on pattern analysis and machine intelligence*, vol. 33, no. 3, pp. 433–445, 2010.

[9] A. Schlögl, F. Lee, H. Bischof, and G. Pfurtscheller, "Characterization of four-class motor imagery eeg data for the bci-competition 2005," *Journal of neural engineering*, vol. 2, no. 4, p. L14, 2005.

[10] B. Liu, X. Huang, Y. Wang, X. Chen, and X. Gao, "Beta: A large benchmark database toward ssvep-bci application," *Frontiers in neuroscience*, vol. 14, p. 627, 2020.

[11] Z. Lin, C. Zhang, W. Wu, and X. Gao, "Frequency recognition based on canonical correlation analysis for ssvep-based bcis," *IEEE transactions on biomedical engineering*, vol. 54, no. 6, pp. 1172–1176, 2007.

[12] X. Chen, Y. Wang, S. Gao, T.-P. Jung, and X. Gao, "Filter bank canonical correlation analysis for implementing a high-speed ssvep-based brain–computer interface," *Journal of neural engineering*, vol. 12, no. 4, p. 046008, 2015.

[13] P. Yuan, X. Chen, Y. Wang, X. Gao, and S. Gao, "Enhancing performances of ssvep-based brain–computer interfaces via exploiting inter-subject information," *Journal of neural engineering*, vol. 12, no. 4, p. 046006, 2015.

[14] M. Nakanishi, Y. Wang, Y.-T. Wang, Y. Mitsukura, and T.-P. Jung, "A high-speed brain speller using steady-state visual evoked potentials," *International journal of neural systems*, vol. 24, no. 06, p. 1450019, 2014.

[15] M. Nakanishi, Y. Wang, X. Chen, Y.-T. Wang, X. Gao, and T.-P. Jung, "Enhancing detection of ssveps for a high-speed brain speller using task-related component analysis," *IEEE Transactions on Biomedical Engineering*, vol. 65, no. 1, pp. 104–112, 2017.

[16] A. Ravi, N. H. Beni, J. Manuel, and N. Jiang, "Comparing user-dependent and user-independent training of cnn for ssvep bci," *Journal of neural engineering*, vol. 17, no. 2, p. 026028, 2020.

[17] R. Luo, X. Xiao, E. Chen, L. Meng, T.-P. Jung, M. Xu, and D. Ming, "Almost free of calibration for ssvep-based brain-computer interfaces," *Journal of Neural Engineering*, vol. 20, no. 6, p. 066013, 2023.

[18] X. Mai, X. Sheng, X. Shu, Y. Ding, X. Zhu, and J. Meng, "A calibration-free hybrid approach combining ssvep and eog for continuous control," *IEEE Transactions on Neural Systems and Rehabilitation Engineering*, 2023.

[19] K.-J. Chiang, C.-S. Wei, M. Nakanishi, and T.-P. Jung, "Boosting template-based ssvep decoding by cross-domain transfer learning," *Journal of Neural Engineering*, vol. 18, no. 1, p. 016002, 2021.

[20] P. R. Bassi, W. Rampazzo, and R. Attux, "Transfer learning and specaugment applied to ssvep based bci classification," *Biomedical Signal Processing and Control*, vol. 67, p. 102542, 2021.

[21] S. J. Pan and Q. Yang, "A Survey on Transfer Learning," *IEEE Transactions on Knowledge and Data Engineering*, vol. 22, no. 10, pp. 1345–1359, 2010.

[22] V. Jayaram, M. Alamgir, Y. Altun, B. Scholkopf, and M. Grosse-Wentrup, "Transfer Learning in Brain-Computer Interfaces Abstract\uFFFDThe performance of brain-computer interfaces (BCIs) improves with the amount of avail," *IEEE Computational Intelligence Magazine*, vol. 11, no. 1, pp. 20–31, 2016.

[23] P. Wang, J. Lu, B. Zhang, and Z. Tang, "A review on trans-

fer learning for brain-computer interface classification," in *2015 5th International Conference on Information Science and Technology (ICIST)*. IEEE, 2015, pp. 315–322.

[24] J. Chen, Y. Zhang, Y. Pan, P. Xu, and C. Guan, "A transformer-based deep neural network model for ssvep classification," *Neural Networks*, vol. 164, pp. 521–534, 2023.

[25] E. Yin, Z. Zhou, J. Jiang, F. Chen, Y. Liu, and D. Hu, "A speedy hybrid bci spelling approach combining p300 and ssvep," *IEEE Transactions on Biomedical Engineering*, vol. 61, no. 2, pp. 473–483, 2014.

[26] E. Yin, T. Zeyl, R. Saab, T. Chau, D. Hu, and Z. Zhou, "A hybrid brain–computer interface based on the fusion of p300 and ssvep scores," *IEEE Transactions on Neural Systems and Rehabilitation Engineering*, vol. 23, no. 4, pp. 693–701, 2015.

[27] E. Yin, Z. Zhou, J. Jiang, F. Chen, Y. Liu, and D. Hu, "A novel hybrid bci speller based on the incorporation of ssvep into the p300 paradigm," *Journal of neural engineering*, vol. 10, no. 2, p. 026012, 2013.

[28] C. M. Wong, Z. Wang, B. Wang, K. F. Lao, A. Rosa, P. Xu, T.-P. Jung, C. P. Chen, and F. Wan, "Inter-and intra-subject transfer reduces calibration effort for high-speed ssvep-based bcis," *IEEE Transactions on Neural Systems and Rehabilitation Engineering*, vol. 28, no. 10, pp. 2123–2135, 2020.

[29] W. Lan, R. Wang, Y. He, Y. Zong, Y. Leng, K. Iramina, W. Zheng, and S. Ge, "Cross domain correlation maximization for enhancing the target recognition of ssvep-based brain-computer interfaces," *IEEE Transactions on Neural Systems and Rehabilitation Engineering*, 2023.

[30] H. Wang, Y. Sun, F. Wang, L. Cao, W. Zhou, Z. Wang, and S. Chen, "Cross-subject assistance: Inter-and intra-subject maximal correlation for enhancing the performance of ssvep-based bcis," *IEEE Transactions on Neural Systems and Rehabilitation Engineering*, vol. 29, pp. 517–526, 2021.

[31] C. M. Wong, Z. Wang, M. Nakanishi, B. Wang, A. Rosa, C. P. Chen, T.-P. Jung, and F. Wan, "Online adaptation boosts ssvep-based bci performance," *IEEE Transactions on Biomedical Engineering*, vol. 69, no. 6, pp. 2018–2028, 2021.

[32] J. Du, Y. Ke, S. Liu, S. Chen, and D. Ming, "Enhancing cross-subject transfer performance for ssvep identification using small data-based transferability evaluation," *Biomedical Signal Processing and Control*, vol. 94, p. 106282, 2024.

[33] J. Lu, V. Behbood, P. Hao, H. Zuo, S. Xue, and G. Zhang, "Transfer learning using computational intelligence: A survey," *Knowledge-Based Systems*, vol. 80, pp. 14–23, 2015.

[34] H. Xiong, J. Song, J. Liu, and Y. Han, "Deep transfer learning-based ssvep frequency domain decoding method," *Biomedical Signal Processing and Control*, vol. 89, p. 105931, 2024.

[35] J. Liu, R. Wang, Y. Yang, Y. Zong, Y. Leng, W. Zheng, and S. Ge, "Convolutional transformer-based cross subject model for ssvep-based bci classification," *IEEE Journal of Biomedical and Health Informatics*, 2024.

[36] J. Huang, Z.-Q. Zhang, B. Xiong, Q. Wang, B. Wan, F. Li, and P. Yang, "Cross-subject transfer method based on domain generalization for facilitating calibration of ssvep-based bcis," *IEEE Transactions on Neural Systems and Rehabilitation Engineering*, 2023.

[37] X. Wang, A. Liu, L. Wu, L. Guan, and X. Chen, "Improving generalized zero-shot learning ssvep classification performance from data-efficient perspective," *IEEE Transactions on Neural Systems and Rehabilitation Engineering*, 2023.

[38] O. B. Guney and H. Ozkan, "Transfer learning of an ensemble of dnns for ssvep bci spellers without user-specific training," *Journal of Neural Engineering*, vol. 20, no. 1, p. 016013, 2023.

[39] R. Vinuesa and B. Sirmacek, "Interpretable deep-learning models to help achieve the sustainable development goals," *Nature Machine Intelligence*, vol. 3, no. 11, pp. 926–926, 2021.

[40] C.-T. Lin and C. G. Lee, *Neural fuzzy systems: a neuro-fuzzy synergism to intelligent systems*. Prentice-Hall, Inc., 1996.

[41] L. Ou, Y.-C. Chang, Y.-K. Wang, and C.-T. Lin, "Fuzzy centered explainable network for reinforcement learning," *IEEE Transactions on Fuzzy Systems*, vol. 32, no. 1, pp. 203–213, 2024.

[42] C.-T. Lin and C. Lee, "Neural-network-based fuzzy logic control and decision system," *IEEE Transactions on Computers*, vol. 40, no. 12, pp. 1320–1336, 1991.

[43] J. Lu, G. Ma, and G. Zhang, "Fuzzy Machine Learning: A Comprehensive Framework and Systematic Review," *IEEE Transactions on Fuzzy Systems*, vol. 32, no. 7, pp. 3861–3878, 2024.

[44] K. Shihabudheen and G. N. Pillai, "Recent advances in neuro-fuzzy system: A survey," *Knowledge-Based Systems*, vol. 152, pp. 136–162, 2018.

[45] Z. Liu, Y. Wang, S. Vaidya, F. Ruehle, J. Halverson, M. Soljačić, T. Y. Hou, and M. Tegmark, "Kan: Kolmogorov-arnold networks," *arXiv preprint arXiv:2404.19756*, 2024.

[46] X. Jiang, L. Ou, Y. Chen, N. Ao, Y.-C. Chang, T. Do, and C.-T. Lin, "A fuzzy logic-based approach to predict human interaction by functional near-infrared spectroscopy," *IEEE Transactions on Fuzzy Systems*, pp. 1–15, 2025.

[47] H. Zuo, G. Zhang, W. Pedrycz, V. Behbood, and J. Lu, "Fuzzy Regression Transfer Learning in Takagi–Sugeno Fuzzy Models," *IEEE Transactions on Fuzzy Systems*, vol. 25, no. 6, pp. 1795–1807, 2017.

[48] H. Zuo, J. Lu, G. Zhang, and W. Pedrycz, "Fuzzy Rule-Based Domain Adaptation in Homogeneous and Heterogeneous Spaces," *IEEE Transactions on Fuzzy Systems*, vol. 27, no. 2, pp. 348–361, 2019.

[49] F. Liu, J. Lu, and G. Zhang, "Unsupervised Heterogeneous Domain Adaptation via Shared Fuzzy Equivalence Relations," *IEEE Transactions on Fuzzy Systems*, vol. 26, no. 6, pp. 3555–3568, 2018.

[50] J. Lu, H. Zuo, and G. Zhang, "Fuzzy Multiple-Source Transfer Learning," *IEEE Transactions on Fuzzy Systems*,

vol. 28, no. 12, pp. 3418–3431, 2020.

[51] X. Zhu, D. Wang, W. Pedrycz, and Z. Li, "Design and Development of Granular Fuzzy Rule-Based Models for Knowledge Transfer," *IEEE Transactions on Systems, Man, and Cybernetics: Systems*, vol. 53, no. 2, pp. 704–715, 2023.

[52] H. Zuo, J. Lu, G. Zhang, and F. Liu, "Fuzzy Transfer Learning Using an Infinite Gaussian Mixture Model and Active Learning," *IEEE Transactions on Fuzzy Systems*, vol. 27, no. 2, pp. 291–303, 2019.

[53] Y.-C. Chang, Y.-K. Wang, N. R. Pal, and C.-T. Lin, "Exploring covert states of brain dynamics via fuzzy inference encoding," *IEEE Transactions on Neural Systems and Rehabilitation Engineering*, vol. 29, pp. 2464–2473, 2021.

[54] T. K. Reddy, Y.-K. Wang, C.-T. Lin, and J. Andreu-Perez, "Joint approximate diagonalization divergence based scheme for eeg drowsiness detection brain computer interfaces," in *2021 IEEE International Conference on Fuzzy Systems (FUZZ-IEEE)*. IEEE, 2021, pp. 1–6.

[55] M. Hu, Y. Zhong, S. Xie, H. Lv, and Z. Lv, "Fuzzy system based medical image processing for brain disease prediction," *Frontiers in Neuroscience*, vol. 15, p. 714318, 2021.

[56] M. F. Zarandi, M. Zarinbal, and M. Izadi, "Systematic image processing for diagnosing brain tumors: A type-ii fuzzy expert system approach," *Applied soft computing*, vol. 11, no. 1, pp. 285–294, 2011.

[57] H. Chen and J. Xie, "EEG-based TSK fuzzy graph neural network for driver drowsiness estimation," *Information Sciences*, vol. 679, p. 121101, 2024.

[58] H. Zuo, G. Zhang, W. Pedrycz, V. Behbood, and J. Lu, "Granular Fuzzy Regression Domain Adaptation in Takagi–Sugeno Fuzzy Models," *IEEE Transactions on Fuzzy Systems*, vol. 26, no. 2, pp. 847–858, 2018.

[59] J. Tahmoresnezhad and S. Hashemi, "Visual domain adaptation via transfer feature learning," *Knowledge and Information Systems*, vol. 50, no. 2, pp. 585–605, 2017.

[60] D. Dubois and H. Prade, "Chapter 6 - pattern classification with fuzzy sets," in *Fuzzy Sets and Systems*, ser. Mathematics in Science and Engineering. Elsevier, 1980, vol. 144, pp. 317–334.

[61] L. Zhang, Y. Shi, Y.-C. Chang, and C.-T. Lin, "Robust fuzzy neural network with an adaptive inference engine," *IEEE Transactions on Cybernetics*, 2023.

[62] V. J. Lawhern, A. J. Solon, N. R. Waytowich, S. M. Gordon, C. P. Hung, and B. J. Lance, "EEGNet: A compact convolutional neural network for EEG-based brain–computer interfaces," *Journal of Neural Engineering*, vol. 15, no. 5, p. 056013, 2018.

[63] A. Vaswani, N. Shazeer, N. Parmar, J. Uszkoreit, L. Jones, A. N. Gomez, L. u. Kaiser, and I. Polosukhin, "Attention is all you need," in *Advances in Neural Information Processing Systems*, I. Guyon, U. V. Luxburg, S. Bengio, H. Wallach, R. Fergus, S. Vishwanathan, and R. Garnett, Eds., vol. 30. Curran Associates, Inc., 2017.

[64] J. Cheng, L. Dong, and M. Lapata, "Long short-term memory-networks for machine reading," 2016.

[65] R. Paulus, C. Xiong, and R. Socher, "A deep reinforced model for abstractive summarization," in *International Conference on Learning Representations*, 2018.

[66] G. R. Müller-Putz, R. Scherer, C. Brauneis, and G. Pfurtscheller, "Steady-state visual evoked potential (ssvep)-based communication: impact of harmonic frequency components," *Journal of neural engineering*, vol. 2, no. 4, p. 123, 2005.

[67] N. R. Waytowich, Y. Yamani, and D. J. Krusienski, "Optimization of checkerboard spatial frequencies for steady-state visual evoked potential brain–computer interfaces," *IEEE Transactions on Neural Systems and Rehabilitation Engineering*, vol. 25, no. 6, pp. 557–565, 2016.

[68] S. Moratti, B. A. Clementz, Y. Gao, T. Ortiz, and A. Keil, "Neural mechanisms of evoked oscillations: stability and interaction with transient events," *Human brain mapping*, vol. 28, no. 12, pp. 1318–1333, 2007.

[69] X. Chen, Y. Wang, M. Nakanishi, X. Gao, T.-P. Jung, and S. Gao, "High-speed spelling with a noninvasive brain–computer interface," *Proceedings of the National Academy of Sciences*, vol. 112, no. 44, 2015.

[70] V. Cherkassky, "Fuzzy inference systems: A critical review," in *Computational Intelligence: Soft Computing and Fuzzy-Neuro Integration with Applications*, O. Kaynak, L. A. Zadeh, B. Türkşen, and I. J. Rudas, Eds. Berlin, Heidelberg: Springer Berlin Heidelberg, 1998, pp. 177–197.

[71] S. R. Chaudhari and M. E. Patil, "Study and review of fuzzy inference systems for decision making and control," in *American International Journal of Research in Science, Technology, Engineering & Mathematics*, 2014.

[72] S. Guillaume, "Designing fuzzy inference systems from data: An interpretability-oriented review," *IEEE Transactions on Fuzzy Systems*, vol. 9, no. 3, pp. 426–443, 2001.

[73] L. Jouffe, "Fuzzy inference system learning by reinforcement methods," *IEEE Transactions on Systems, Man, and Cybernetics, Part C (Applications and Reviews)*, vol. 28, no. 3, pp. 338–355, 1998.

[74] J. R. Wolpaw, N. Birbaumer, D. J. McFarland, G. Pfurtscheller, and T. M. Vaughan, "Brain–computer interfaces for communication and control," *Clinical Neurophysiology*, vol. 113, no. 6, pp. 767–791, 2002.

[75] M. Koch, D. M. Mittleman, J. Ornik, and E. Castro-Camus, "Terahertz time-domain spectroscopy," *Nature Reviews Methods Primers*, vol. 3, no. 1, p. 48, 2023.

[76] A. Luo and T. J. Sullivan, "A user-friendly ssvep-based brain–computer interface using a time-domain classifier," *Journal of neural engineering*, vol. 7, no. 2, p. 026010, 2010.

[77] L. Ou, T. Do, X.-T. Tran, D. Leong, Y.-C. Chang, Y.-K. Wang, and C.-T. Lin, "Improving cca algorithms on ssvep classification with reinforcement learning based temporal filtering," in *Australasian Joint Conference on Artificial Intelligence*. Springer, 2023, pp. 376–386.